

Many Body Effects on Electron Tunneling through Quantum Dots in an AB Circuit

## Many Body Effects on Electron Tunneling through Quantum Dots in an Aharonov-Bohm Circuit

Wataru IZUMIDA,\* Osamu SAKAI and Yukihiro SHIMIZU<sup>1</sup>

*Department of Physics, Tohoku University, Sendai 980-77, Japan*

<sup>1</sup>*Department of Applied Physics, Tohoku University, Sendai 980-77, Japan*

(Received October 15, 1996)

Tunneling conductance of an Aharonov-Bohm circuit including two quantum dots is calculated based on the general expression of the conductance in the linear response regime of the bias voltage. The calculation is performed in a wide temperature range by using numerical renormalization group method. Various types of AB oscillations appear depending on the temperature and the potential depth of the dots. Especially, AB oscillations have strong higher harmonics components as a function of the magnetic flux when the potential of the dots is deep. This is related to the crossover of the spin state due to the Kondo effect on quantum dots. When the temperature rises up, the amplitude of the AB oscillations becomes smaller reflecting the breaking of the coherency.

KEYWORDS: quantum dots, Aharonov-Bohm effect, Kondo effect, numerical renormalization group method

---

\* izumida@cmpt01.phys.tohoku.ac.jp

## §1. Introduction

There are many systems that electron-electron interactions play important roles in the physical properties of them. A system of metal with dilute magnetic impurities is a good example. Various anomalous phenomena are observed at low temperatures, related to the Kondo effect, which is caused by competition between quantum coherence effects and electron-electron interactions.<sup>1)</sup>

In the phenomenon of the electron tunneling through a quantum dot between leads, the effects of the electron-electron interactions in the dot have been investigated extensively.<sup>2, 3, 4, 5, 6, 7, 8, 9, 10, 11, 12)</sup> The importance of the Kondo effect in a quantum dot has been pointed out by some theoreticians.<sup>2, 3, 4, 5, 6, 7, 8, 9)</sup> The ‘Kondo effect in a quantum dot’ will give the following features. In low temperatures than the Kondo temperature of the system,  $T_K$ , the conductance will show the coherent resonant tunneling caused by the Kondo resonance peak in the quantum dot. When the temperature rises up than  $T_K$ , the Kondo resonance peak vanishes and the local spin freedom appears, and so the electron tunneling with inelastic spin scattering process will dominate. Therefore the coherent resonant tunneling process will be broken.

The interference phenomenon is the good indication for the coherency of the electronic state. The Aharonov-Bohm (AB) circuits with quantum dots have been investigated to study the coherency on quantum dots.<sup>13, 14, 15, 16, 17, 18)</sup> Akera had studied the system in which two quantum dots are included in AB circuit, and shown that the amplitude of the AB oscillations depends on the spin state of the dots.<sup>13)</sup> However, his investigation was restricted only to the high temperature region than  $T_K$ . Main purpose of the present work is to study how the Kondo effect affects the AB oscillations. We calculate the temperature dependence of the AB oscillations in a wide temperature range including the crossover temperature  $T_K$ .

In this paper, we consider the system shown in Fig. 1, which is the same system that Akera studied. The essential physics of this system can be given by the two impurity Anderson Hamiltonian. Because our interests are related to the change of the coherency of the electronic state, we have to calculate the conductance without assumptions on tunneling processes. In other words, the assumption, such as the restriction to the ‘coherent resonant tunneling process’ or to the ‘sequential tunneling process’, should not be used. Numerical Renormalization Group (NRG) method has been known as a useful method to study the many body systems written by the Anderson Hamiltonian.<sup>19, 20, 21)</sup> This method has reliability in the temperature range near and below  $T_K$ . In this paper, we develop this method to calculate the conductance without assumptions on tunneling processes.

Main results of this paper are as follows: When the temperature rises up, the amplitude of the AB oscillations becomes smaller reflecting breaking of the coherency by spin inelastic scattering; Various types of AB oscillations appear due to many body effects when the depth of dot’s potential is changed; AB oscillations have strong higher harmonics components as a function of the magnetic

Fig. 1. The geometry of the two quantum dots and leads. Electron tunneling from the one lead to the other lead can occur only via quantum dots. The magnetic flux  $\Phi$  is applied between leads and dots to cause AB interference effect.

flux reflecting the crossover of the spin state.

In section 2, the model Hamiltonian of the system is given and is transformed for numerical calculation. The conductance formula is derived based on the linear response theory. At the same time, for comparisons, the conductance formula based on the coherent resonant tunneling process is derived by using the Friedel sum rule. In section 3, numerical results of the conductance are shown. In section 4, summary and discussion of this study are given.

## §2. Formulation

### 2.1 Model and transformation

For simplicity, we consider following situation for our system in Fig. 1. Energy separations between states of the single-electron orbits in a dot are much larger than the other energy scales: the Coulomb repulsion energy  $U$ , temperature  $T$ , and the level width  $\Delta$ . This situation corresponds to the assumption that only one single-electron orbit in the dot contributes to the current. Two electrons can occupy in this orbit because of the spin degeneracy, but the second electron need excess energy  $U$  due to the Coulomb interaction between two electrons. The orbit in the dot couples to those in leads, and this causes the electron tunneling. Tunneling from the one lead to the other lead can occur only via quantum dots. The essential properties of the system can be written by the Anderson model as follows;

$$H = H_1 + H_d + H_{1-d}, \quad (2.1)$$

$$H_1 = \sum_{\vec{k}\sigma} \varepsilon_{a\vec{k}\sigma} a_{\vec{k}\sigma}^\dagger a_{\vec{k}\sigma} + \sum_{\vec{p}\sigma} \varepsilon_{b\vec{p}\sigma} b_{\vec{p}\sigma}^\dagger b_{\vec{p}\sigma}, \quad (2.2)$$

$$H_d = \sum_{i=1,2} \sum_{\sigma} \varepsilon_{d,i} d_{i\sigma}^\dagger d_{i\sigma} + \sum_{i=1,2} U_i d_{i\uparrow}^\dagger d_{i\uparrow} d_{i\downarrow}^\dagger d_{i\downarrow}, \quad (2.3)$$

$$\begin{aligned}
H_{1-d} = & \sum_{\vec{k}\sigma} (v_{a\vec{k},1} e^{i\frac{\varphi}{4}} d_{1\sigma}^\dagger a_{\vec{k}\sigma} + v_{a\vec{k},2} e^{-i\frac{\varphi}{4}} d_{2\sigma}^\dagger a_{\vec{k}\sigma} + h.c.) \\
& + \sum_{\vec{p}\sigma} (v_{b\vec{p},1} e^{-i\frac{\varphi}{4}} d_{1\sigma}^\dagger b_{\vec{p}\sigma} + v_{b\vec{p},2} e^{i\frac{\varphi}{4}} d_{2\sigma}^\dagger b_{\vec{p}\sigma} + h.c.),
\end{aligned} \tag{2.4}$$

where  $a_{\vec{k}\sigma}$  is the annihilation operator of the electron with spin  $\sigma$  and the state  $\vec{k}$  in the left lead A,  $b_{\vec{p}\sigma}$  is that of in the right lead B, and  $d_{i,\sigma}$  is that of on the orbit in the  $i$ -th dot, respectively. The quantity  $\varepsilon_{d,i}$  is the single-electron level of orbit in the  $i$ -th dot, and is the effective depth of dot's potential. The quantity  $U_i$  is the Coulomb repulsion energy in the  $i$ -th dot. The terms  $H_1$  and  $H_d$  denote the leads and the dots, respectively, and  $H_{1-d}$  is the electron tunneling term between leads and dots. The factor  $e^{\pm i\frac{\varphi}{4}}$  is due to the magnetic flux. ( $\varphi = 2\pi\Phi/\Phi_0$ , where  $\Phi$  is the magnetic flux enclosed by the circuit, and  $\Phi_0$  is the magnetic flux quantum,  $hc/e$ .)

We transform the model Hamiltonian to fit numerical calculation. We consider only the situation that  $\varepsilon_{d,1} = \varepsilon_{d,2} \equiv \varepsilon_d$  and  $U_1 = U_2 \equiv U$  for simplicity. Furthermore, we assume that the geometry of the leads has symmetry with respect to the interchange of dot 1 and dot 2. Moreover we also assume the symmetry with respect to the interchange of lead A and lead B. Electron motion in the leads are restricted only to the one-dimensional motion along the lead. (The state index  $\vec{k}$  is reduced to  $k$ .) Neglecting the  $k$  dependence of the tunneling matrix, we put the relations,  $v_{ak,1} = v_{bp,1} = v_{ak,2} = v_{bp,2} \equiv V$ . Finally, each term is rewritten as

$$H_1 = \sum_{k\sigma} \varepsilon_k (\alpha_{s,k\sigma}^\dagger \alpha_{s,k\sigma} + \alpha_{a,k\sigma}^\dagger \alpha_{a,k\sigma}), \tag{2.5}$$

$$\begin{aligned}
H_d = & \varepsilon_d (\sum_{\sigma} n_{e,\sigma} + \sum_{\sigma} n_{o,\sigma}) \\
& + \frac{U}{2} (n_{e,\uparrow} n_{e,\downarrow} + n_{o,\uparrow} n_{o,\downarrow}) \\
& + \frac{U}{4} (n_{e,\uparrow} + n_{e,\downarrow}) (n_{o,\uparrow} + n_{o,\downarrow}) \\
& - \frac{U}{4} \sum_{\sigma_1 \sigma_2 \sigma_3 \sigma_4} (\vec{\sigma})_{\sigma_1 \sigma_2} \cdot (\vec{\sigma})_{\sigma_3 \sigma_4} d_{e,\sigma_1}^\dagger d_{e,\sigma_2} d_{o,\sigma_3}^\dagger d_{o,\sigma_4} \\
& - \frac{U}{2} (d_{e,\uparrow}^\dagger d_{e,\downarrow}^\dagger d_{o,\downarrow} d_{o,\uparrow} + d_{o,\uparrow}^\dagger d_{o,\downarrow}^\dagger d_{e,\downarrow} d_{e,\uparrow}),
\end{aligned} \tag{2.6}$$

$$\begin{aligned}
H_{1-d} = & 2 \sum_{k\sigma} (V \cos \frac{\varphi}{4} d_{e,\sigma}^\dagger \alpha_{s,k\sigma} + V \sin \frac{\varphi}{4} d_{o,\sigma}^\dagger \alpha_{a,k\sigma} \\
& + h.c.),
\end{aligned} \tag{2.7}$$

where  $\alpha_{s,k\sigma} \equiv (a_{k\sigma} + b_{k\sigma})/\sqrt{2}$  is the symmetric combination of the lead orbits, and  $\alpha_{a,k\sigma} \equiv (a_{k\sigma} - b_{k\sigma})/\sqrt{2}$  is the anti-symmetric combination of those, and  $d_{e,\sigma} \equiv (d_{1\sigma} + d_{2\sigma})/\sqrt{2}$ ,  $d_{o,\sigma} \equiv -i(d_{1\sigma} - d_{2\sigma})/\sqrt{2}$  are those of the dot orbits, respectively. The quantity  $\vec{\sigma}$  is the Pauli matrix. The problem is reduced to solve the two-channel Anderson model as seen in eqs. (2.5), (2.6) and (2.7). Hereafter, we call the orbit denoted by  $d_{e,\sigma}$  as 'even-orbit' and the channel of it as 'even-channel', and those

of  $d_{o,\sigma}$  as ‘odd-orbit’ and ‘odd-channel’. We denote them by  $l$  as  $l = e$  or  $l = o$ .

## 2.2 Conductance formula

In this paper, we restrict ourselves to the linear response conductance for the applied bias voltage. We derive the conductance formula without assumptions on electron tunneling processes. We also derive the conductance formula with assumption of the coherent resonant tunneling process. Calculated results are compared at very low temperature.

### 2.2.1 Conductance formula at finite temperature

Now, we must calculate the conductance without using approximations for tunneling processes such as the sequential tunneling process picture or the coherent tunneling process picture. We define an electric current from lead A to lead B as follows;

$$I \equiv -e \frac{-\langle \dot{N}_A \rangle + \langle \dot{N}_B \rangle}{2}, \quad (2.8)$$

where  $-e$  is the charge of an electron, and  $\langle \dot{N}_A \rangle$  is the expectation value of the time differentiation of  $N_A = \sum_{k\sigma} a_{k\sigma}^\dagger a_{k\sigma}$ , the electron number operator in the lead A. The quantity  $\langle \dot{N}_B \rangle$  is that of the lead B. We consider the situation applying the voltage  $2V$  between lead A and lead B. This situation is given by adding the term  $H' = N_A eV - N_B eV$  to our Hamiltonian  $H$ , eq. (2.1). Assuming that the voltage difference  $2V$  is small, and using linear response theory derived by Kubo,<sup>22)</sup> we obtain the following expression for the conductance formula (see Appendix);

$$\begin{aligned} G &\equiv \frac{I}{2V} \\ &= \frac{2e^2}{h} \lim_{\omega \rightarrow 0} \frac{P''(\omega)}{\omega}, \end{aligned} \quad (2.9)$$

with

$$\begin{aligned} P''(\omega) &= \frac{\pi^2 \hbar^2}{4} \frac{1}{Z} \sum_{n,m} \left( e^{-\beta E_m} - e^{-\beta E_n} \right) \\ &\quad \times \left| \langle n | \dot{N}_A - \dot{N}_B | m \rangle \right|^2 \\ &\quad \times \delta(\omega - (E_n - E_m)), \end{aligned} \quad (2.10)$$

where  $Z = \sum_n e^{-\beta E_n}$  is the partition function,  $\beta = 1/T$ ,  $T$  is the temperature of the system.

The quantities  $\langle \dot{N}_A \rangle$  and  $\langle \dot{N}_B \rangle$  can be expressed by localized operators near the dots as shown in Appendix. So, this expression is suitable for the numerical calculation by the NRG method, though it needs the delicate limiting process  $\omega \rightarrow 0$ .

### 2.2.2 Conductance formula at zero temperature based on the coherent resonant tunneling process

Here we derive the conductance formula at zero temperature for comparison with numerical results from eqs. (2.9) and (2.10). The conductance at zero temperature is given by

$$G_F = \frac{2\pi e^2}{\hbar} \sum_{\sigma, S_{\text{int}}} \sum_{\sigma', S_{\text{fin}}} |T_{\text{fin,int}}(\epsilon_F)|^2$$

$$\times \rho^2(\varepsilon_F) W_{S_{\text{int}}}, \quad (2.11)$$

where initial and final states of transition are denoted as  $\text{int} = (k\sigma, S_{\text{int}})$  and  $\text{fin} = (p\sigma', S_{\text{fin}})$ . The quantity  $k$  denotes the electron in the lead A, and  $p$  denotes that in the lead B. By  $S_{\text{int}}$  and  $S_{\text{fin}}$  we represent initial and final states on the quantum dots, and  $W_{S_{\text{int}}}$  is the probability of state in  $S_{\text{int}}$ . The quantity  $T_{\text{fin, int}}$  is the transition matrix, and  $\rho(\varepsilon_F)$  is the density of states on the Fermi energy in the leads. The transition matrix is written by using Green's function  $\mathcal{G}$  as  $T = V + V\mathcal{G}V$ , where  $V = H_{1-d}$  in this case.

At zero temperature, the system written in eq. (2.1) is expected to be in the local Fermi liquid state. Electron tunneling processes through the quantum dots will be given by only the coherent resonant tunneling process, i.e.,  $S_{\text{int}} = S_{\text{fin}}$ . The conductance  $G_F$  is written as follows;

$$G_F = \frac{2e^2}{h} |\Delta_e \mathcal{G}_{e,\sigma}(\varepsilon_F + i0) - \Delta_o \mathcal{G}_{o,\sigma}(\varepsilon_F + i0)|^2, \quad (2.12)$$

with

$$\Delta_e = 4\pi |V|^2 \rho(\varepsilon_F) \cos^2 \frac{\varphi}{4}, \quad (2.13)$$

$$\Delta_o = 4\pi |V|^2 \rho(\varepsilon_F) \sin^2 \frac{\varphi}{4}. \quad (2.14)$$

In the local Fermi liquid state, Green's function  $\mathcal{G}_{l,\sigma}(\varepsilon_F + i0)$  in the  $l$ -th channel ( $l = e, o$ ) satisfies the Friedel sum rule as follows<sup>23, 24</sup>;

$$\mathcal{G}_{l,\sigma}(\varepsilon_F + i0) = \frac{1}{\left(-\Delta_l \frac{1}{\tan \delta_l} + i\Delta_l\right)}, \quad (2.15)$$

where  $\delta_l$  is the phase shift for the  $l$ -th channel. Using the relation between the phase shift  $\delta_l$  and the ground-state occupation number  $\langle n_{0,l} \rangle$  on the  $l$ -th orbit,

$$\langle n_{0,l} \rangle = 2 \frac{\delta_l}{\pi}, \quad (2.16)$$

we get the conductance as follows;

$$G_F = \frac{2e^2}{h} \sin^2 \left\{ \frac{\pi}{2} (\langle n_{0,e} \rangle - \langle n_{0,o} \rangle) \right\}. \quad (2.17)$$

Although the expression (2.17) seems to be different from eq. (2.9), it can be derived from eq. (2.9) when the system is in the local Fermi liquid state and  $T = 0$ .

The expression (2.17) is contrast with the single dot case. In such a case, the conductance is given by  $(2e^2/h) \sin^2(\pi \langle n_0 \rangle / 2)$ , and it has almost the maximum value  $2e^2/h$  when there is the Kondo resonance peak on the Fermi energy, i.e.,  $\langle n_0 \rangle \sim 1$ .<sup>2, 3, 4</sup> On the other hand, the conductance has very small value in the present case as seen from (2.17) if the even and odd components have simultaneously the Kondo resonance on the Fermi energy, i.e.,  $\langle n_{0,e} \rangle \sim \langle n_{0,o} \rangle \sim 1$ . This is caused by the interference cancellation between processes through the even and odd orbit states.

### 2.3 Excitation spectra

We will calculate excitation spectra other than  $P''(\omega)$  to get insights of the electronic states of the dots system. The single particle excitation spectrum for the  $l$ -th orbit ( $l = e, o$ ) is defined as follows;

$$\begin{aligned} \rho_l(\omega) \equiv & \frac{1}{Z} \sum_{n,m} \left( e^{-\beta E_m} - e^{-\beta E_n} \right) \\ & \times \left( \left| \langle n | d_l^\dagger | m \rangle \right|^2 \delta(\omega - (E_n - E_m)) \right. \\ & \left. + \left| \langle n | d_l | m \rangle \right|^2 \delta(\omega + (E_n - E_m)) \right). \end{aligned} \quad (2.18)$$

The magnetic excitation spectrum at  $T = 0$  is calculated as follows;

$$\begin{aligned} \chi''_{m,e}(\omega) \equiv & \sum_n \sum_{\text{Gr}} \left| \langle n | (S_{e,z} + S_{o,z}) | \text{Gr} \rangle \right|^2 \\ & \times \delta(\omega - (E_n - E_{\text{Gr}})), \end{aligned} \quad (2.19)$$

where  $S_{l,z} = (d_{l,\uparrow}^\dagger d_{l,\uparrow} - d_{l,\downarrow}^\dagger d_{l,\downarrow})/2$  is the spin operator on the  $l$ -th orbit and Gr denotes the ground state of the system. The energy of the peak position will reflect the characteristic energy of the spin fluctuation. In this paper, the energy of the peak position of  $\chi''_{m,e}(\omega)$  is used as the definition of the Kondo temperature,  $T_K$ . For the four fold degenerate model, this definition gives rather well approximate value of  $T_K$  defined by the usual definition based on the susceptibility.<sup>20)</sup>

### §3. Numerical Results

We have several parameters for the model. The band width of the leads,  $D$ , is chosen to be energy units,  $D = 1$ . The parameters  $\varepsilon_d, U, \Delta \equiv 4\pi|V|^2\rho(\varepsilon_F)$  and  $T$  are given in units of  $D$ .

In this paper, we fix the Coulomb repulsion energy to be  $U = 0.10$  and the tunneling intensity  $\Delta = 0.03\pi$ . It is enough to study the only  $\varepsilon_d \geq -0.5U$  cases because the conductance as a function of  $\varepsilon_d$  is symmetric with respect to  $\varepsilon_d = -0.5U$ . Then the energy level  $\varepsilon_d$  is varied from  $-0.05 = -0.50U$ , corresponding to the electron-hole symmetric case, to  $0.1 = 1.0U$ . The conductance is the periodic function of the magnetic flux  $\varphi$  and moreover it is even function of  $\varphi$  for the present model, so we calculate the conductance only in a half period,  $0 \leq \varphi \leq \pi$ . Temperature  $T$  is varied from  $5.8 \times 10^{-7}$  to  $3.1 \times 10^{-1}$ . (See Table I and II.)

Before going to detailed discussions of the numerical results, we stress the following fact. The Kondo effects in different channels seem to occur as if they are independent though the original Hamiltonian includes interaction terms between electrons in even and odd orbits. (See eq. (2.6).) As shown later in §3.2, the Kondo resonance peaks of the single particle excitation in even-channel do not have structure reflecting the energy scale of the odd-channel Kondo effect, and *vice versa*.

Table I. Parameters  $\varepsilon_d$ ,  $U$ ,  $\Delta \equiv 4\pi|V|^2\rho(\varepsilon_F)$  in units of the band width  $D$ .

$\varepsilon_d$	$U$	$\Delta/\pi$
$-0.050 = -0.50U$		
$-0.030 = -0.30U$		
$-0.025 = -0.25U$		
$-0.020 = -0.20U$	0.10	0.03
$+0.000 = +0.00U$		
$+0.050 = +0.50U$		
$+0.100 = +1.00U$		

Table II. Temperatures denoted as  $T_i$  in this paper. These are given in units of the band width  $D$ .

$T_1$	$T_2$	$T_3$	$T_4$	$T_5$	$T_6$	$T_7$
$5.8 \times 10^{-7}$	$1.7 \times 10^{-6}$	$5.2 \times 10^{-6}$	$1.6 \times 10^{-5}$	$4.7 \times 10^{-5}$	$1.4 \times 10^{-4}$	$4.2 \times 10^{-4}$
$T_8$	$T_9$	$T_{10}$	$T_{11}$	$T_{12}$	$T_{13}$	
$1.3 \times 10^{-3}$	$3.8 \times 10^{-3}$	$1.1 \times 10^{-2}$	$3.4 \times 10^{-2}$	$1.1 \times 10^{-1}$	$3.1 \times 10^{-1}$	

### 3.1 Conductance at zero temperature $G_F(\varphi)$

The conductance at zero temperature is written by using the difference of the occupation numbers,  $\langle n_{0,e} \rangle - \langle n_{0,o} \rangle$ , as shown in eq. (2.17). The expectation value of the occupation number  $\langle n_{0,l} \rangle$  is calculated from the wave function obtained by the NRG method, and is shown in Fig. 2. In the electron-hole symmetric case,  $\varepsilon_d = -0.050$ , the expectation values satisfy the relation  $\langle n_{0,e} \rangle = \langle n_{0,o} \rangle = 1.0$  for any  $\varphi$ . When  $\varepsilon_d$  moves away from  $\varepsilon_d = -0.050$ , both  $\langle n_{0,e} \rangle$  and  $\langle n_{0,o} \rangle$  deviate from 1.0 and they depend on the flux  $\varphi$ . We note that the hybridization strength for the odd-orbit,  $\Delta_o = 4\pi|V|^2\rho(\varepsilon_d)\sin^2(\varphi/4)$ , is very small in the  $\varphi \sim 0$  region. Therefore the small change



Fig. 2. The expectation values of the occupation number of the even-orbit,  $\langle n_{0,e} \rangle$ , and the odd-orbit,  $\langle n_{0,o} \rangle$ , in the ground state as a function of  $\varphi$  for various cases of  $\varepsilon_d$ . The flux  $\varphi$  is given in units of  $\Phi_0 = hc/e$ . The value  $\langle n_{0,o} \rangle$  at  $\varphi \sim 0$  decreases rapidly as  $\varepsilon_d$  increases between  $\varepsilon_d = -0.025$  to  $-0.020$ .

of the parameters in a critical region causes drastic change of the ground state properties of the odd-channel. Reflecting these,  $\langle n_{0,o} \rangle$  at  $\varphi \sim 0$  decreases rapidly as  $\varepsilon_d$  increases from  $-0.025$  to  $-0.020$ . At the same time the Kondo resonance peak in the odd-channel rapidly moves away from the Fermi energy.

We have two regimes for the  $\varphi$ -dependence of  $\langle n_{0,o} \rangle$ . In the  $\varepsilon_d \leq -0.025$  case,  $\langle n_{0,o} \rangle$  has value almost 1.0 at  $\varphi \sim 0$ . It initially decreases with increasing  $\varphi$ , and then increases gradually. In the  $\varepsilon_d \geq -0.020$  case,  $\langle n_{0,o} \rangle$  has very small value at  $\varphi \sim 0$ . It increases with increasing  $\varphi$ . In contrast to the behavior of  $\langle n_{0,o} \rangle$ , the occupation number  $\langle n_{0,e} \rangle$  shows mild dependence on  $\varepsilon_d$  and  $\varphi$  because the hybridization strength  $\Delta_e$  is relatively large in  $0 \leq \varphi \leq \pi$  region.

In Fig. 3, we present the numerical results of the conductance at zero temperature  $G_F(\varphi)$

for various  $\varepsilon_d$ . The AB oscillations vanish completely in the electron-hole symmetric case,<sup>25)</sup>

Fig. 3. The conductance at zero temperature,  $G_F(\varphi)$ , for various cases of  $\varepsilon_d$ . The units of  $G_F(\varphi)$  is  $2e^2/h$ . In the electron-hole symmetric case ( $\varepsilon_d = -0.50U = -0.050$ ), AB oscillations vanish completely. As  $\varepsilon_d$  shifts from  $\varepsilon_d = -0.050$ , the AB oscillations appear. The conductance  $G_F(\varphi)$  near  $\varphi = 0$  increases rapidly when  $\varepsilon_d$  increases from  $\varepsilon_d = -0.025$  to  $-0.020$ .

$\varepsilon_d = -0.050$ , because  $\langle n_{0,e} \rangle = \langle n_{0,o} \rangle = 1$  as noted in Fig. 2. When  $\varepsilon_d$  moves away from  $\varepsilon_d = -0.050$ , the AB oscillations appear because the quantity  $\langle n_{0,e} \rangle - \langle n_{0,o} \rangle$  has non zero value and depends on the flux  $\varphi$ .

We note that  $G_F(\varphi)$  near  $\varphi \sim 0$  increases rapidly as  $\varepsilon_d$  increases between  $\varepsilon_d = -0.025$  to  $-0.020$ . This phenomenon is reflecting the behavior of  $\langle n_{0,o} \rangle$ . In the region of  $\langle n_{0,o} \rangle \sim 0$ , the Kondo resonance peak of the odd-channel moves away from the Fermi energy. Therefore, the contribution of the resonant tunneling via the Kondo resonance of the odd-channel becomes very small. From this we can see that the conductance  $G_F(\varphi = 0)$  take value near  $2e^2/h$  when only the coherent resonant tunneling of the even-channel contributes.

To conclude, the AB oscillations of the conductance at zero temperature show two types of  $\varphi$  dependence reflecting the change of the ground state properties of the system. In the  $\varepsilon_d \leq -0.025$  case,  $G_F(\varphi)$  is very small at  $\varphi \sim 0$ . It decreases initially and soon increases with  $\varphi$ , and then it decreases near  $\varphi/\pi \sim 1$  after showing maximum. In other word, the AB oscillations have higher harmonics components. On the other hand in  $\varepsilon_d \geq -0.020$  case,  $G_F(\varphi)$  has large value at  $\varphi = 0$ , and it decreases with  $\varphi$ .

### 3.2 Conductance at finite temperature $G(\varphi)$

In this subsection we show the numerical results of the conductance  $G(\varphi)$  at various temperatures calculated by eqs. (2.9) and (2.10).

In Fig. 4, we show examples of the spectra,  $P''(\omega)/\omega$ , calculated by the NRG method. The

Fig. 4. Examples of the spectrum,  $P''(\omega)/\omega$ , calculated by using the NRG method. The parameters are  $\varepsilon_d = -0.025$  and  $T = T_5 (= 4.7 \times 10^{-5})$ . The symbols give the NRG raw data points, and lines are given by spline interpolation. The edge of the lines give the lowest energy data points for the interpolation,  $|\omega_{\min}| = 4.0T_5$ . The data points  $\omega/T < \alpha \sim 1$  should be discarded in the NRG calculation, see the text.

calculated raw data are plotted by symbols, and the lines give the values averaged by the spline interpolation method. The data points with energies  $\omega/T < \alpha \sim 1$  are expected to be erroneous because they are calculated from transitions with excitation energy ( $T \sim |t_L|$ ) larger than  $\omega$ , where  $|t_L|$  is the hopping matrix characterizing the low energy scale of the NRG calculation.<sup>20,21)</sup> In the interpolation, these low energy data are discarded. The value at  $\omega_{\min} = 4.0T$  is substituted for the limiting value of  $\omega \rightarrow 0$ . As shown from Fig. 4, this process does not lead the ambiguity of the limiting value of  $P''(\omega)/\omega$  for the low temperature cases  $T \ll T_K$ . But it causes ambiguity for the  $T > \alpha' \sim T_K$  cases. The quantitative accuracy of the numerical value of the present work should not be so trusted for higher temperature cases. However, it seems not bad for the qualitative discussions.

In the following subsections, we show two typical cases for the numerical results of the conductance at finite temperature.

### 3.2.1 Deep $\varepsilon_d$ case ( $\varepsilon_d = -0.025$ )

Numerical results of the conductance  $G(\varphi)$  at  $\varepsilon_d = -0.025$  for various temperatures are shown in Fig. 5.

Fig. 5. The conductance  $G(\varphi)$  at  $\varepsilon_d = -0.025$  for various temperatures. The regions given by the broken lines are the magnetic state and the regions given by the solid lines are the non-magnetic state. For the definition, see the text. The curves of the conductance given by the solid line region for  $T_1 \leq T \leq T_7$  cases coincide to  $G_F(\varphi)$  of  $\varepsilon_d = -0.025$  case in Fig. 3. Tunneling processes are expected to be dominated by the coherent resonant tunneling process on solid lines. On broken lines, contributions from the process with the spin inelastic scattering will be not so small. The conductance rapidly changes at  $\varphi/\pi \sim 0.10$  in the temperature cases  $T_1 \leq T \leq T_7$ . For the origin of this phenomena, see also the text.

First, we discuss the results in the temperature range  $T_1 \leq T \leq T_7$ . The conductance  $G(\varphi)$  changes rapidly as  $\varphi$  changes between  $0.1 < \varphi/\pi < 0.3$ . In addition, it has value near  $2e^2/h$  in  $\varphi/\pi < 0.1$  region contrasted to the result of  $G_F(\varphi)$  for  $\varepsilon_d = -0.025$  in Fig. 3. In the region of  $\varphi/\pi > 0.3$ , the curves of the conductance  $G(\varphi)$  overlap to each other, and also coincide with the result from  $G_F(\varphi)$ .

To get insights the origin of this behavior of the conductance, we investigate the electronic state of the system. The one-particle excitation spectra  $\pi\Delta_e\rho_e(\omega)$  and  $\pi\Delta_o\rho_o(\omega)$ , and also the current spectra  $P''(\omega)$  for various flux cases at  $T = T_1$  are shown in Fig. 6. The same quantities at  $T = T_3$  are shown in Fig. 7. At  $T = T_1$ , we have the Kondo resonance peaks in the even-channel for all flux  $\varphi$  cases. (Notice that the abscissa have a logarithmic scale.) On the other hand in  $\varphi/\pi < 0.1$  cases for the odd-channel, the widths of the Kondo resonance peaks are small compared to the lowest energy calculated in the Fig. 6. The width gradually increases as flux  $\varphi$  increases from  $\varphi/\pi \sim 0.10$ , and the complete Kondo resonance peak appears in the  $\varphi/\pi > 0.15$  cases.

Fig. 6. Excitation spectra  $\pi\Delta_e\rho_e(\omega)$ ,  $\pi\Delta_o\rho_o(\omega)$ , and  $P''(\omega)/\omega$  at  $T = T_1$  and  $\varepsilon_d = -0.025$ . The Kondo resonance peaks on Fermi energy always exist in  $\rho_e(\omega)$ . On the other hand, There are no Kondo resonance peaks in  $\rho_o(\omega)$  when  $\varphi/\pi < 0.1$ . The Kondo resonance peaks in  $\rho_o(\omega)$  gradually grow up as flux increases from  $\varphi/\pi \sim 0.1$ . The peaks appear completely in the  $\varphi/\pi > 0.15$  region.

The evolution of the Kondo resonance peak in a certain channel means that the electronic state in the channel is in the spin singlet state. In this case, the excitation properties will be described as the Fermi liquid state. Therefore, the electron tunneling processes through that channel will be given by only the coherent resonant tunneling process.

The even-channel state is always in the Fermi liquid state at  $T = T_1$  for whole range of  $\varphi$ . The electronic state of the odd-channel falls into the Fermi liquid state for  $\varphi/\pi > 0.15$  at  $T = T_1$ . On the other hand for the cases  $\varphi/\pi < 0.1$ , the spin state of the odd-channel at  $T = T_1$  is expected to be magnetic. Fig. 7 shows the spectra at  $T = T_3$ . The intensity of the Kondo resonance of odd-channel with  $\varphi/\pi = 0.141$  decreases remarkably from the lines in Fig. 6. At the same time the conductance increases.

It may be advisable to consider the Kondo temperature,  $T_K$ , for given  $\varphi$  case. Now, we define

Fig. 7. Excitation spectra  $\pi\Delta_e\rho_e(\omega)$ ,  $\pi\Delta_o\rho_o(\omega)$ , and  $P''(\omega)/\omega$  at  $T = T_3$  and  $\varepsilon_d = -0.025$ . The Kondo resonance peaks in  $\rho_o(\omega)$  appear in the  $\varphi/\pi > 0.25$  region. The region of  $\varphi$  that the odd-channel being magnetic state becomes wider when the temperature rises as seen from comparison with Fig. 6.

$T_K(\varphi)$  as an energy of the peak position of the magnetic excitation spectrum at zero temperature  $\chi''_{m,e}(\omega)$  given by eq. (2.19). The result is shown in Fig. 8. In the figure we also show the spectrum  $\chi''_{m,e}(\omega)$  for several values of  $\varphi$ . The energy of the peak position is expected to reflect the characteristic energy of the spin fluctuation on the odd-channel. For  $\varphi/\pi = 0.125$ , we have peak at  $\omega/D = 5.2 \times 10^{-6}$  and the energy of the peak position increases rapidly as  $\varphi$  increases. For the cases  $\varphi/\pi < 0.125$ , the peak position shift to very low energy, and thus we can not show it in the frame of the figure.

The judgments of the boarder between the magnetic state (broken lines) to non-magnetic state (solid lines) in Fig. 5 were given by using  $T_K(\varphi)$  in Fig. 8. Tunneling processes are expected to occur by the coherent resonant tunneling process in the solid line region. On the broken lines, the contribution from the processes with the inelastic spin excitation will be not small. The conductance show relatively large difference from  $G_F(\varphi)$  in this region.

Fig. 8. The Kondo temperature  $T_K(\varphi)$  as a function of the magnetic flux  $\varphi$  at  $\varepsilon_d = -0.025$ . Inset data are the magnetic excitation spectra at zero temperature. The energies  $\omega$  of the peak positions of the spectra are used for the definition of  $T_K(\varphi)$ .  $T_K(\varphi \sim 0)$  is extremely low because the hybridization intensity of the odd-channel,  $\Delta_o$ , is proportional to  $\sin^2(\varphi/4)$  and is very small for  $\varphi \sim 0$ .  $T_K(\varphi)$  increases as  $\varphi$  increases from  $\varphi = 0$  to  $\pi$ .

When the temperature  $T$  rises beyond  $T_7$ , the conductance near  $\varphi/\pi \sim 1$  gradually increases and the AB oscillations become relatively smaller. When the temperature increases further through  $T_{10} = 1.1 \times 10^{-2}$ , the conductance near  $\varphi/\pi \sim 0$  gradually decreases and the AB oscillations become very small.<sup>26)</sup> The spin states of both even and odd channels gradually change from non-magnetic to magnetic state for  $\varphi/\pi \sim 1$  as temperature rises up.

We can conclude that the behavior of the conductance strongly reflects the spin state in the quantum dots. At this place we comments on the difference of  $G(\varphi)$  at very low temperature  $T = T_1$  from the curve of  $G_F(\varphi)$  at exactly zero temperature. The conductance  $G_F(\varphi = 0)$  is less than  $0.1 \times 2e^2/h$ , but  $G(\varphi = 0)$  is almost  $2e^2/h$  even at very low temperature  $T = T_1$ . In our calculation, it is very difficult to get the results which agree with  $G_F(\varphi)$  in the region  $\varphi/\pi < 0.15$ , because we must continue the numerical computation to extremely low energy region. We have checked that calculations up to low energy region  $\omega \sim 10^{-7}$ ,  $T \sim 10^{-8}$  gives consistent result with  $G_F(\varphi)$  for  $\varphi/\pi = 0.117$ . (See Fig. 9). But it is impossible to continue such calculation to  $\varphi/\pi < 0.117$  cases. In the  $\varphi/\pi < 0.15$  cases at  $T = T_1$ , the contribution from the coherent resonant tunneling process of the odd-channel will be small because  $T_K(\varphi)$  is less than  $T_1$ . In such cases, the conductance will have the value near  $2e^2/h$  as seen from Fig. 3. We think that abrupt increase of  $G(\varphi \sim 0)$  at  $T = T_1$  from  $G_F(\varphi \sim 0)$  really reflects the crossover of states due to the increase of the temperature.

Fig. 9. The excitation spectra  $P''(\omega)/\omega$  at the temperature  $T = T_1 = 5.8 \times 10^{-7}$  (left figure) and  $T = 2.1 \times 10^{-8}$  (right figure) at  $\varphi/\pi = 0.117$ ,  $\varepsilon_d = -0.025$ . The spectrum  $P''(\omega)/\omega$  at  $T = 2.1 \times 10^{-8}$  gives consistent result with  $G_F(\varphi/\pi = 0.117) = 2.4 \times 10^{-3}$  at  $\varepsilon_d = -0.025$ .

Here, we note the meaning of the spectrum  $P''(\omega)/\omega$ . This quantity is related to the fluctuation of the bias voltage. It shows peak structure at energy comparable to the width of the Kondo resonance at the Fermi energy. It shows two peaks structure when  $\varphi$  is small, as clearly seen in Fig. 9. These peaks seem to relate to the Kondo resonance in each channel.

### 3.2.2 Shallow $\varepsilon_d$ case ( $\varepsilon_d = 0.000$ )

Numerical results of the conductance  $G(\varphi)$  at  $\varepsilon_d = 0.000$  for various  $T$  are shown in Fig. 10. The conductance  $G(\varphi)$  does not show rapid changes in this case, contrasted to the results shown in Fig. 5. We show the Kondo temperature  $T_K(\varphi)$  in the  $\varepsilon_d = 0.000$  case in Fig. 11. It is much higher than that of  $\varepsilon_d = -0.025$  case in Fig. 8 at  $\varphi \sim 0$ . In the  $\langle n_{0,o} \rangle \sim 0.0$  case, spin freedom on the odd-orbit will disappear and so the spin excitation mainly comes from the electrons in the even-orbit. Then the Kondo temperature  $T_K(\varphi)$  is larger in this case. Even when the occupation number on odd-orbit increases due to the increase of  $\varphi$ , the characteristic magnetic excitation energy is not so small because the electrons in both channels are in the mixed valence regime. So the variation of  $T_K(\varphi)$  for change of  $\varphi$  is much smaller than that in the  $\varepsilon_d = -0.025$  case. Therefore the conductance in Fig. 10 does not show the rapid change caused by the crossover of the spin state. In the temperature range  $T < T_9$ , the conductance shows simple  $\cos \varphi$  like behavior contrasted to the complicated  $\varphi$  dependence of  $\varepsilon_d = -0.025$  case. When the temperature  $T$  rises up than  $T_{10}$ , the AB oscillations become smaller because the temperature becomes comparable to  $T_K(\varphi)$ .<sup>26)</sup>



Fig. 10. The conductance  $G(\varphi)$  for various temperatures at  $\varepsilon_d = 0.000$ . AB oscillations become smaller as temperature rises up than  $T \sim T_9$ . The phenomenon that  $G(\varphi)$  rapidly changes with flux at low temperatures can not be seen in this case.

#### §4. Summary and Discussion

In this paper, we have investigated the temperature and the magnetic flux dependences of the conductance  $G$  for the AB circuit including two quantum dots. This quantity is expected to reflect the coherency of the electronic state, and is closely related to the ‘Kondo effect in quantum dots’. The model Hamiltonian had the form of the two-channel Anderson model with even and odd orbits. The conductance was calculated by using the NRG method based on the formula without assumptions on tunneling processes.

There were interaction terms between electrons in even and odd orbits, but the Kondo effects in the even-channel and the odd-channel occurred as if they were independent. When the dots system were in the Kondo regime near  $\varphi \sim 0$ , i.e., the occupation number in the odd-orbit satisfies  $\langle n_{0,o} \rangle \sim 1.0$ , the crossover of the spin state in the odd-channel occurred at a critical value of  $\varphi$  at low temperature. This is because the hybridization strength of odd-channel increases from the small value near  $\varphi \sim 0$  to large value with increasing  $\varphi$ . AB oscillations had strong higher harmonics components reflecting the crossover of the spin state of the system. This result was contrasted to the single  $\cos \varphi$  dependence derived by Akera.<sup>13)</sup> When the temperature rose up very high, the amplitude of the AB oscillations became smaller as expected. When the dots system were in the mixed valence regime near  $\varphi \sim 0$ , i.e.,  $\langle n_{0,o} \rangle \sim 0.0$ , the drastic change of the conductance as a function of  $\varphi$  did not occur.

At this place, we remark limitation of the assumptions used to derive the simplified expressions, eqs. (2.5), (2.6) and (2.7). The even and odd channels were separated out, and the hybridization

Fig. 11. The Kondo temperature  $T_K(\varphi)$  as a function of the magnetic flux  $\varphi$  at  $\varepsilon_d = 0.000$  case. Inset data are the magnetic excitation spectra at zero temperature. The energies  $\omega$  of the peak positions of the spectra are used for the definition of  $T_K(\varphi)$ . The variation of  $T_K(\varphi)$  for the change of  $\varphi$  is smaller when compared with result for  $\varepsilon_d = -0.025$  case.

of odd-channel is proportional to  $\sin(\varphi/4)$ . This led the drastic change of the electronic state of the odd-channel near  $\varphi \sim 0$ . However, if the dot 1 and dot 2 are asymmetric under the interchange of them, electrons in both channels mix with each other. Therefore, the  $\varphi$ -dependence near  $\varphi \sim 0$  will be blurred in the asymmetric case. The experimental work of Yacoby *et al.* has been done in this situation.<sup>14, 15)</sup> Extension of our calculation to the asymmetric cases will be given in near future. We stress that the present work treated the case that most drastic changes of the tunneling conductance are expected.

Anyway, the conductance will show sharp  $\varphi$ -dependence reflecting the crossover of the spin state of dots, when the Kondo effect is caused by the suitable variation of the dot potential energy.

### Acknowledgments

The authors would like to thank H. Akera for valuable discussions and information, and R. Takayama for helpful advice in numerical computation. The numerical computation was performed at the Computer Center of Institute for Molecular Science, the Computer Center of Tohoku University and the Supercomputer Center of Institute for Solid State.

## Appendix: Formulation of the conductance in the linear response theory

We define an electric current as follows;

$$I \equiv -e \frac{-\langle \dot{N}_A \rangle + \langle \dot{N}_B \rangle}{2}, \quad (\text{A}\cdot 1)$$

where  $-e$  is the charge of an electron. The quantity  $\dot{N}_A \equiv \frac{i}{\hbar}[H, N_A]$  is the time derivative of the electron number operator in the lead A,  $N_A = \sum_{k\sigma} a_{k\sigma}^\dagger a_{k\sigma}$ , and  $\dot{N}_B$  is that in the lead B.

We consider the current when the external perturbation term  $H' = -N_A V_A - N_B V_B$  is added to  $H$  which is given by eq. (2.1). The expectation values,  $\langle \dot{N}_A \rangle$  and  $\langle \dot{N}_B \rangle$  are given within the linear response theory,<sup>22)</sup>

$$\langle \dot{N}_A \rangle = \sigma_{AA} V_A + \sigma_{AB} V_B, \quad (\text{A}\cdot 2)$$

$$\langle \dot{N}_B \rangle = \sigma_{BA} V_A + \sigma_{BB} V_B, \quad (\text{A}\cdot 3)$$

with

$$\sigma_{\mu\nu} = \lim_{\omega \rightarrow 0} \sigma_{\mu\nu}(\omega) \quad (\text{A}\cdot 4)$$

$$\begin{aligned} &\equiv \lim_{\omega \rightarrow 0} \frac{i}{\hbar} \left\{ \int_0^\infty dt' e^{-\delta t' + i\omega t'} \right. \\ &\quad \left. \times \text{Tr} \left( e^{-i\frac{H}{\hbar}t'} [N_\nu, \rho_{\text{eq}}] e^{i\frac{H}{\hbar}t'} \dot{N}_\mu \right) \right\}, \end{aligned} \quad (\text{A}\cdot 5)$$

where  $\delta = 0+$ . Using properties of the trace operator and integration by parts, we get the following expression;

$$\sigma_{\mu\nu}(\omega) = \frac{1}{i\omega} (K_{\mu\nu}(\omega) - K_{\mu\nu}(0)), \quad (\text{A}\cdot 6)$$

with

$$K_{\mu\nu}(\omega) \equiv -\frac{i}{\hbar} \int_0^\infty e^{-\delta t + i\omega t} \langle [\dot{N}_\nu, \dot{N}_\mu(t)] \rangle dt. \quad (\text{A}\cdot 7)$$

The quantity  $K_{\mu\nu}(\omega)$  can be expressed by the following form;

$$K_{\mu\nu}(\omega) = K'_{\mu\nu}(\omega) + iK''_{\mu\nu}(\omega), \quad (\text{A}\cdot 8)$$

where  $K'_{\mu\nu}(\omega)$  and  $K''_{\mu\nu}(\omega)$  are given as follows by using the eigenstates of  $H$  (i.e.,  $H|m\rangle = E_m|m\rangle$ ),

$$\begin{aligned} K'_{\mu\nu}(\omega) &= \frac{1}{Z} \sum_{n,m} \left( e^{-\beta E_n} - e^{-\beta E_m} \right) \\ &\quad \times \frac{E_m - E_n + \hbar\omega}{(E_m - E_n + \hbar\omega)^2 + (\hbar\delta)^2} \\ &\quad \times \langle n | \dot{N}_\nu | m \rangle \langle m | \dot{N}_\mu | n \rangle \end{aligned} \quad (\text{A}\cdot 9)$$

$$= K'_{\mu\nu}(-\omega), \quad (\text{A}\cdot 10)$$

$$\begin{aligned}
K''_{\mu\nu}(\omega) &= \frac{1}{Z} \sum_{n,m} \left( e^{-\beta E_n} - e^{-\beta E_m} \right) \\
&\quad \times \frac{-\hbar\delta}{(E_m - E_n + \hbar\omega)^2 + (\hbar\delta)^2} \\
&\quad \times \langle n | \dot{N}_\nu | m \rangle \langle m | \dot{N}_\mu | n \rangle
\end{aligned} \tag{A.11}$$

$$= -K''_{\mu\nu}(-\omega). \tag{A.12}$$

The quantity  $\sigma_{\mu\nu}$  is given by

$$\sigma_{\mu\nu} = \lim_{\omega \rightarrow 0} \frac{K''_{\mu\nu}(\omega)}{\omega}. \tag{A.13}$$

We give the value  $-V_A = -eV$  and  $-V_B = eV$  for external field, and obtain the electric current as follows;

$$I = \frac{e^2}{4} (\sigma_{AA} + \sigma_{BB} - \sigma_{AB} - \sigma_{BA}) \cdot 2V. \tag{A.14}$$

The conductance  $G$  is given by

$$G \equiv \frac{I}{2V} \tag{A.15}$$

$$= \frac{2e^2}{h} \lim_{\omega \rightarrow 0} \frac{P''(\omega)}{\hbar\omega}, \tag{A.16}$$

with

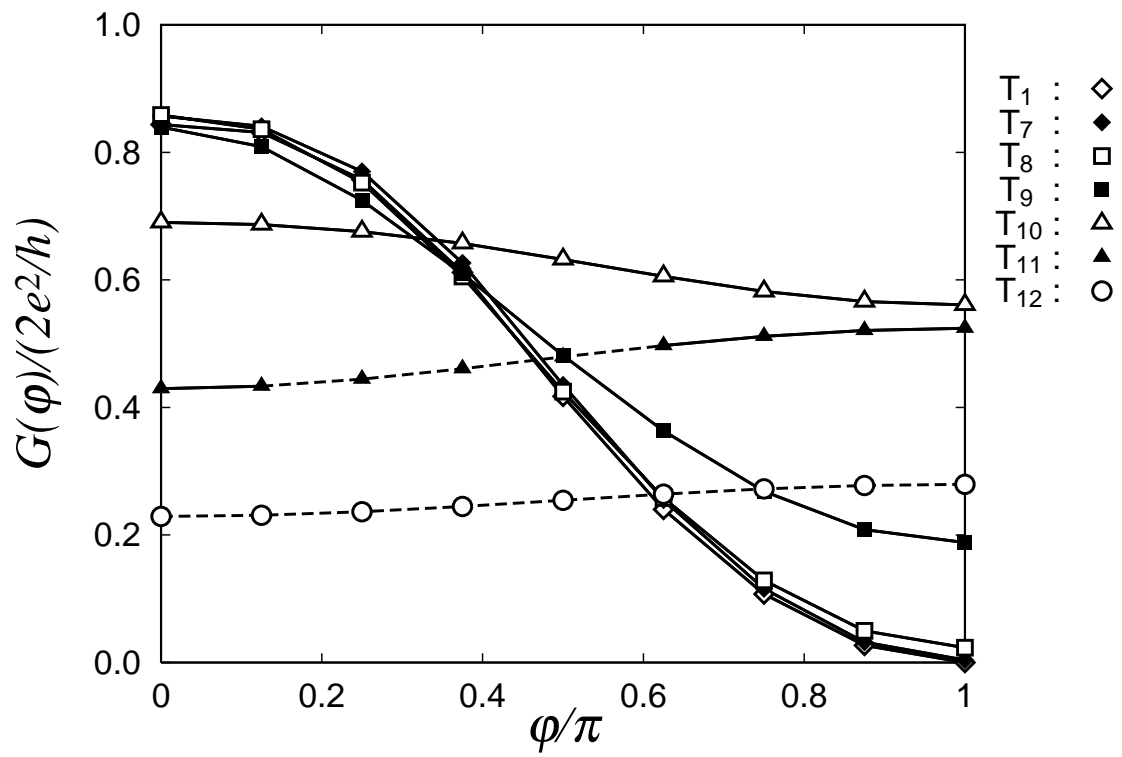
$$\begin{aligned}
P''(\omega) &\equiv \frac{\pi^2 \hbar^2}{4} \frac{1}{Z} \sum_{n,m} \left( e^{-\beta E_m} - e^{-\beta E_n} \right) \\
&\quad \times \left| \langle n | \dot{N}_A - \dot{N}_B | m \rangle \right|^2 \\
&\quad \times \delta(\hbar\omega - (E_n - E_m)).
\end{aligned} \tag{A.17}$$

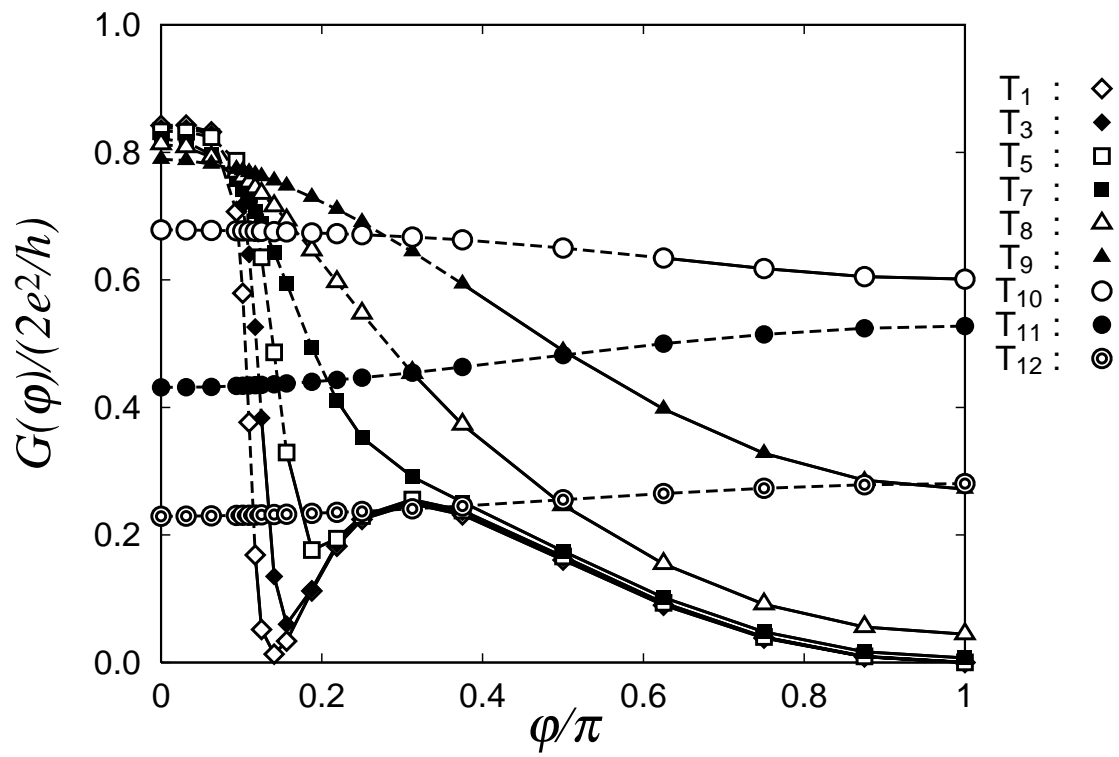
We note that the operator  $\dot{N}_\mu$  ( $\mu = A, B$ ) can be expressed by the localized operators near the dots. For example,  $\dot{N}_A - \dot{N}_B$  is given as follows;

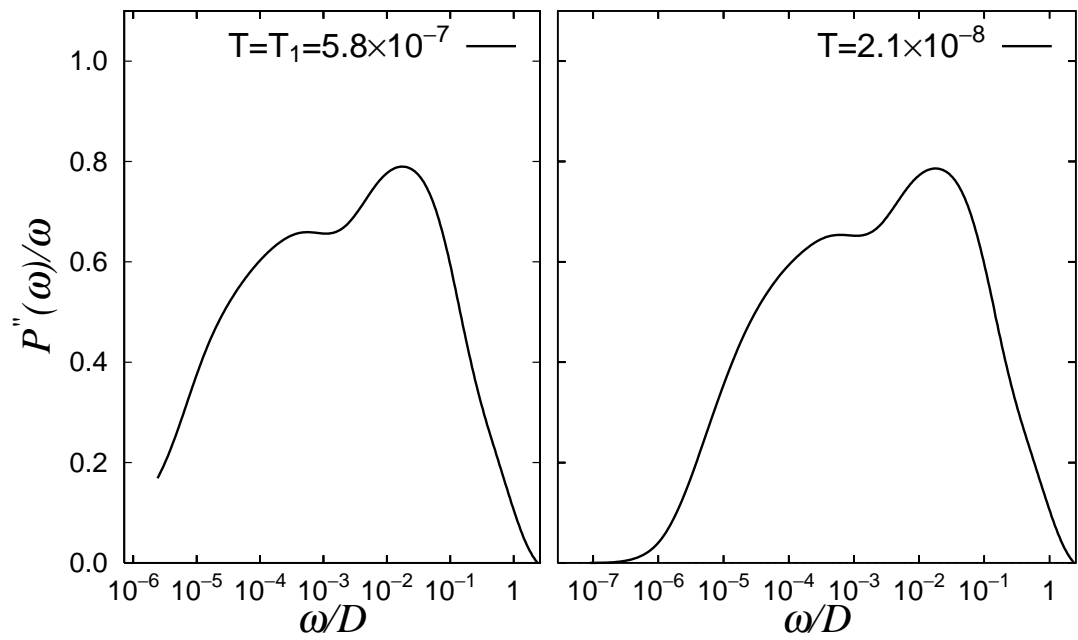
$$\begin{aligned}
\dot{N}_A - \dot{N}_B &= \frac{2i}{\hbar} \sum_{k\sigma} V \left( \cos \frac{\varphi}{4} d_{e,\sigma}^\dagger \alpha_{a,k\sigma} \right. \\
&\quad \left. + \sin \frac{\varphi}{4} d_{o,\sigma}^\dagger \alpha_{s,k\sigma} - h.c. \right).
\end{aligned} \tag{A.18}$$

In this place the operator  $\sum_{k\sigma} \alpha_{l,k\sigma}$  ( $l = s, a$ ), which is given by linear combination of all  $k$ -state, is proportional to the localized orbit near the dots. Therefore the expression of conductance by using the quantity  $P''(\omega)$  is suitable for the calculation based on the NRG method, in which the approximate eigenstates are obtained successively starting from the localized orbits.

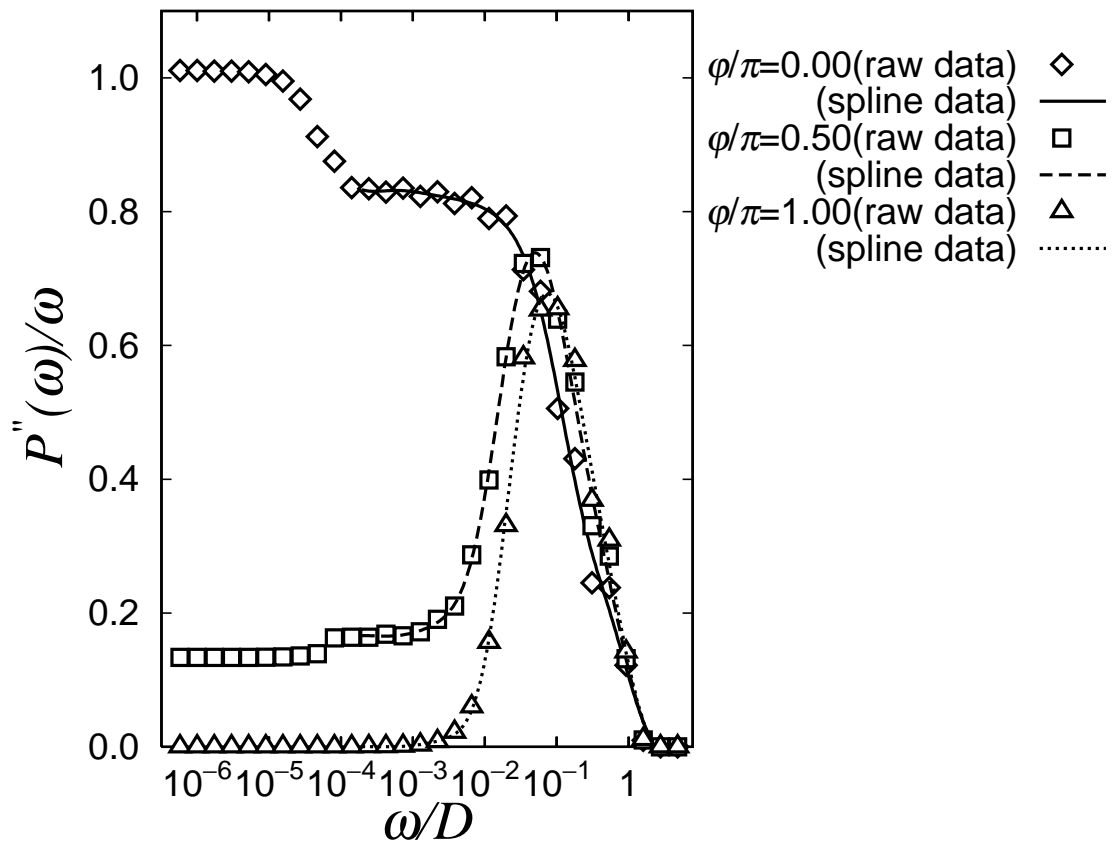
- 
- [1] See for example, A. C. Hewson: *The Kondo problem to Heavy Fermions* (Cambridge University Press, Cambridge, 1993) and references cited therein.
- [2] T. K. Ng and P. A. Lee: Phys. Rev. Lett. **61** (1988) 1768.
- [3] L. I. Glazman and M. É. Raïkh: JETP Lett. **47** (1988) 452.
- [4] A. Kawabata: J. Phys. Soc. Jpn. **60** (1991) 3222.
- [5] A. Oguri, H. Ishii and T. Saso: Phys. Rev. B **51** (1995) 4715.
- [6] S. Hershfield, J. H. Davies and J. W. Wilkins: Phys. Rev. Lett. **67** (1991) 3720.
- [7] Y. Meir, N. S. Wingreen and P. A. Lee: Phys. Rev. Lett. **70** (1993) 2601.
- [8] A. L. Yeyati, A. Martín-Rodero and F. Flores: Phys. Rev. Lett. **71** (1993) 2991.
- [9] T. Inoshita, A. Shimizu, Y. Kuramoto and H. Sasaki: Phys. Rev. B **48** (1993) 14725.
- [10] L. I. Glazman and K. A. Matveev: JETP Lett. **51** (1990) 485.
- [11] Y. Meir, N. S. Wingreen and P. A. Lee: Phys. Rev. Lett. **66** (1991) 3048.
- [12] A. Groshev, T. Ivanov and V. Valtchinov: Phys. Rev. Lett. **66** (1991) 1082.
- [13] H. Akera: Phys. Rev. B **47** (1993) 6835.
- [14] A. Yacoby, M. Heiblum, D. Mahalu, and H. Shtrikman: Phys. Rev. Lett. **74** (1995) 4047.
- [15] A. Yacoby, R. Schuster, and M. Heiblum: Phys. Rev. B **53** (1996) 9583.
- [16] A. L. Yeyati and M. Büttiker: Phys. Rev. B **52** (1995) 14360.
- [17] G. Hackenbroich and H. A. Weidenmüller: Phys. Rev. Lett. **76** (1996) 110.
- [18] C. Bruder, R. Fazio, and H. Shoeller: Phys. Rev. Lett. **76** (1996) 114.
- [19] H. R. Krishnamurthy, J. W. Wilkins and K. G. Wilson: Phys. Rev. B **21** (1980) 1003; **21** (1980) 1044.
- [20] O. Sakai, S. Suzuki and Y. Shimizu: Physica B **206 & 207** (1995) 141.
- [21] Y. Shimizu and O. Sakai: *Computational Physics as a New Frontier in Condensed Matter Research* ed. H. Takayama, M. Tsukada, H. Shiba, F. Yonezawa, M. Imada and Y. Okabe (The Physical Society of Japan, 1995) p.42.
- [22] R. Kubo: J. Phys. Soc. Jpn. **12** (1957) 570.
- [23] D. C. Langreth: Phys. Rev. **150** (1966) 516.
- [24] H. Shiba: Prog. Theor. Phys. **54** (1975) 967.
- [25] In general, there is no reason to be  $\langle n_{0,e} \rangle = \langle n_{0,o} \rangle = 1$ . This result is critically dependent on the assumption that the hybridization of each channel has electron-hole symmetry. In realistic cases, AB oscillations with small amplitude are expected.
- [26] For the temperatures higher than  $T_K$ , and in the parameters region  $\varepsilon_d < \varepsilon_F < \varepsilon_d + U$ , one can find that the conductance is proportional to  $(K^2 + 4J^2 \langle \vec{S}_1 \cdot \vec{S}_2 \rangle) \cos \varphi + C$ , where  $K = (1/\varepsilon_d + 1/(\varepsilon_d + U))$ ,  $J = (1/\varepsilon_d - 1/(\varepsilon_d + U))$  and  $C$  is constant in  $\varphi$ . (This expression is obtained following Akera's consideration.<sup>13</sup>) Usually we can expect  $4J^2 \gg K^2$  and  $\langle \vec{S}_1 \cdot \vec{S}_2 \rangle < 0$ , so the coefficient of  $\cos \varphi$  could have the negative sign. The numerical results in  $T \geq T_{11}$  might be shown in such a case.

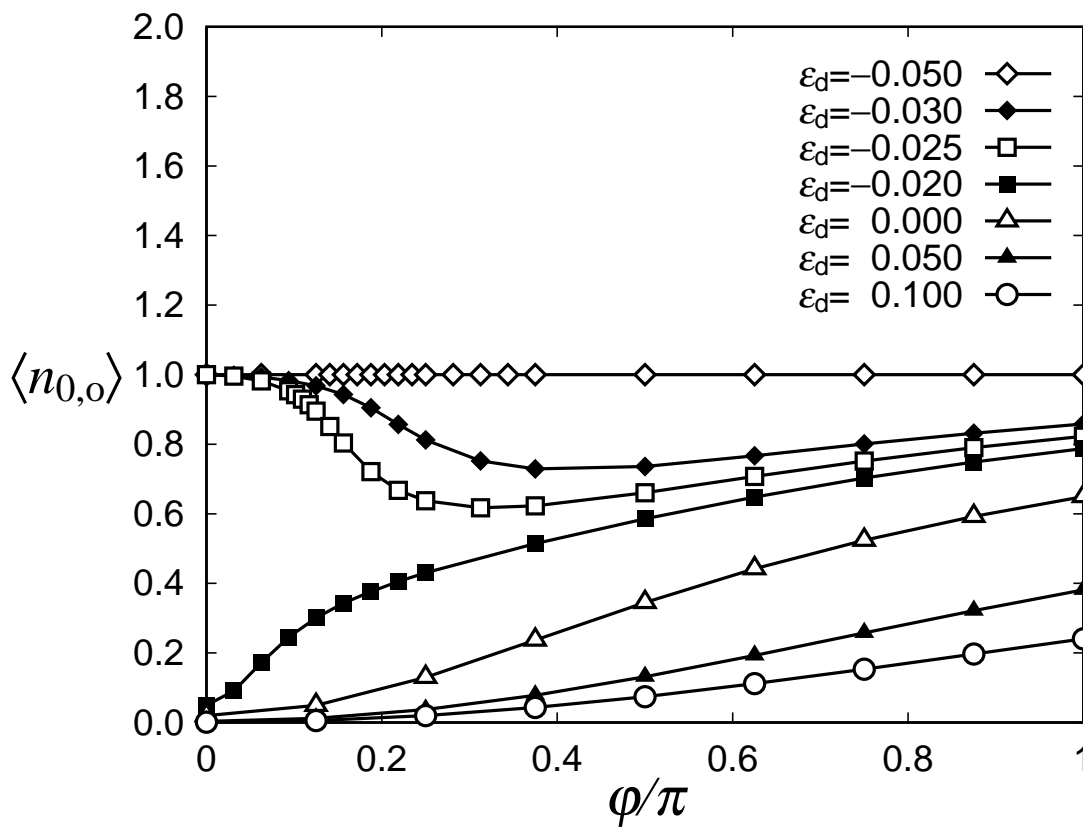
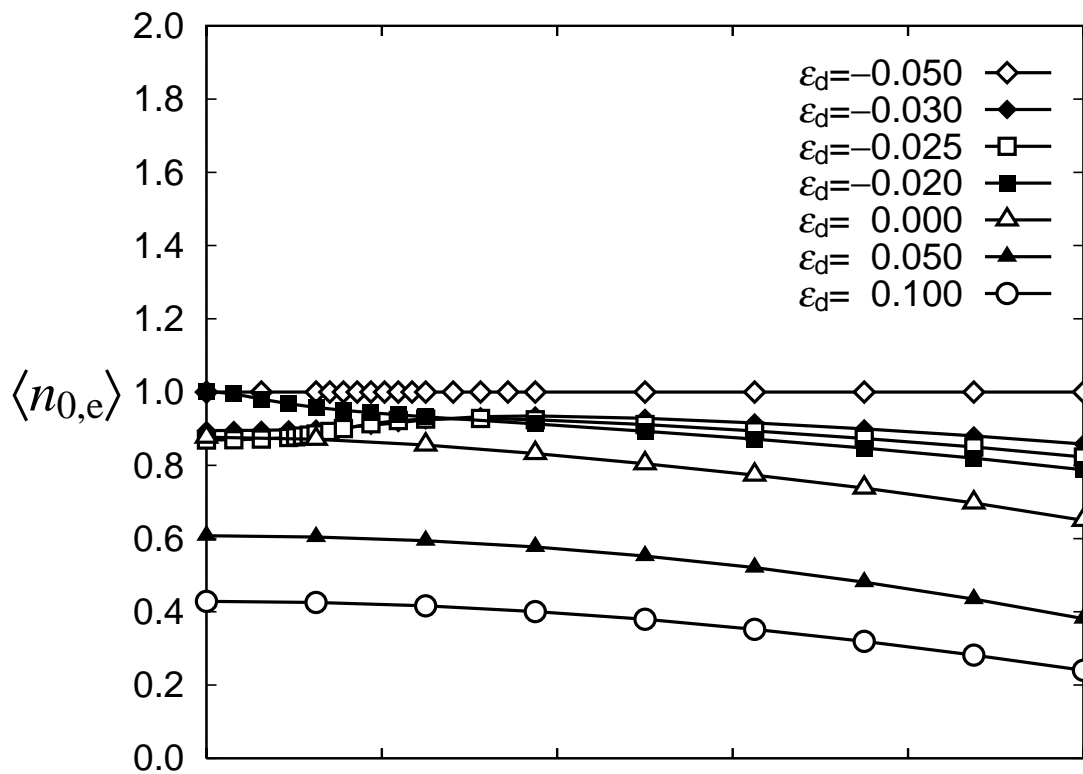




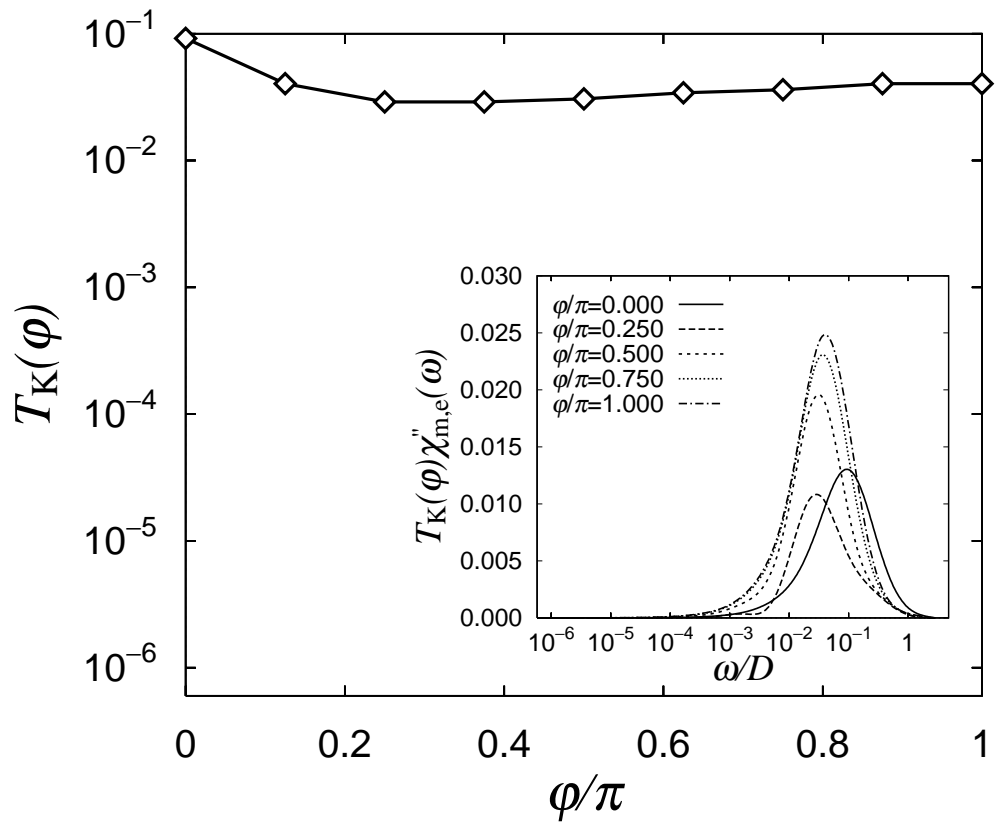


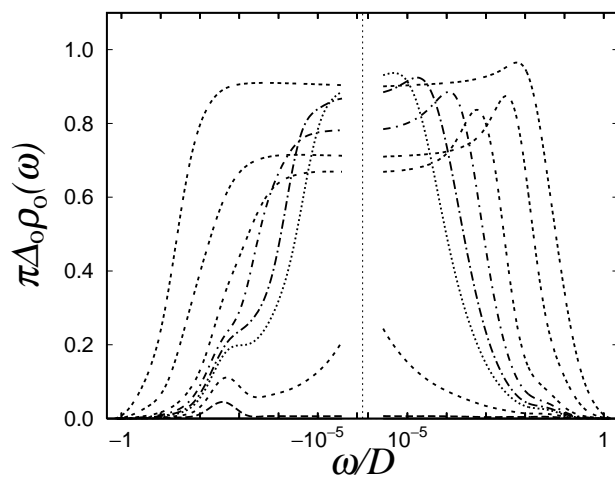
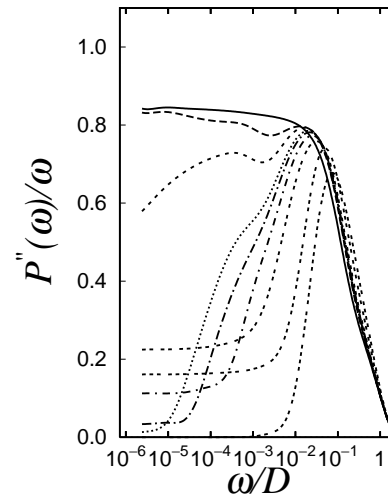
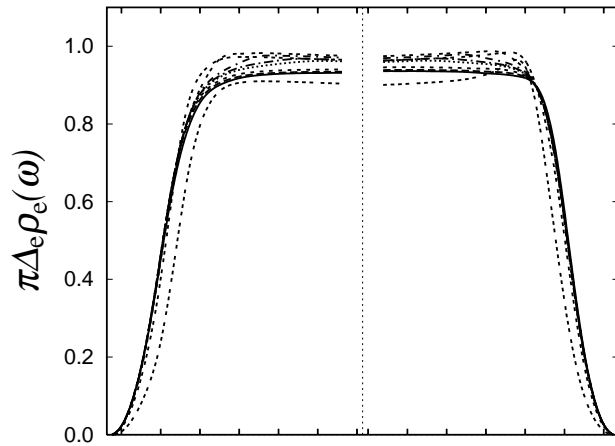




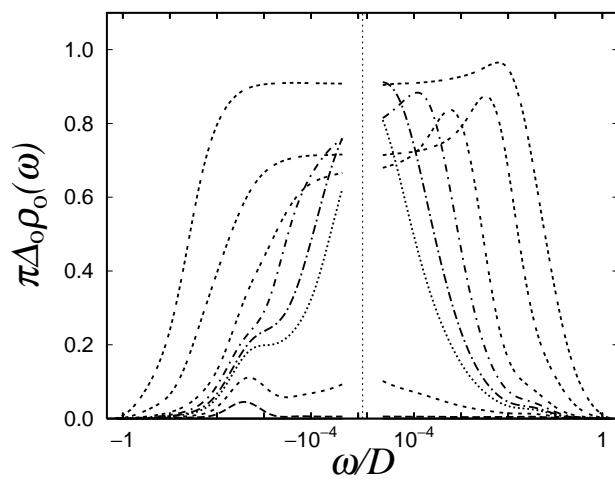
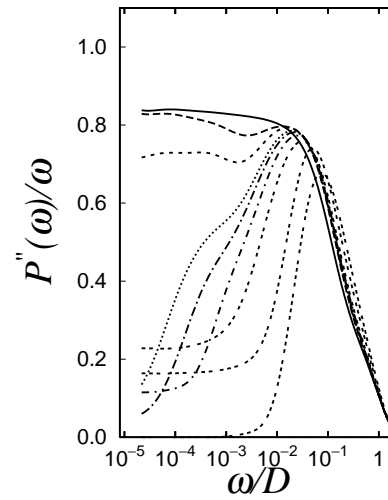
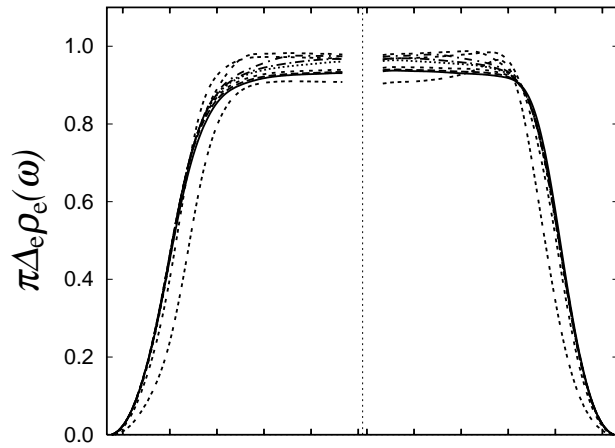








- $\phi/\pi=0.000$  ———
- $\phi/\pi=0.062$  - - - -
- $\phi/\pi=0.102$  ·····
- $\phi/\pi=0.141$  -·-·-
- $\phi/\pi=0.156$  - - - -
- $\phi/\pi=0.188$  -·-·-
- $\phi/\pi=0.250$  - - - -
- $\phi/\pi=0.500$  ·····
- $\phi/\pi=1.000$  -·-·-



- $\phi/\pi=0.000$  ———
- $\phi/\pi=0.062$  - - - -
- $\phi/\pi=0.102$  ·····
- $\phi/\pi=0.141$  ·····
- $\phi/\pi=0.156$  - - - -
- $\phi/\pi=0.188$  ·····
- $\phi/\pi=0.250$  ·····
- $\phi/\pi=0.500$  ·····
- $\phi/\pi=1.000$  ·····

